JOURNAL OF CHEMICAL INFORMATION AND MODELING

Article

pubs.acs.org/jcim

Modeling Androgen Receptor Flexibility: A Binding Mode Hypothesis of CYP17 Inhibitors/Antiandrogens for Prostate Cancer Therapy

Eleonora Gianti[†] and Randy J. Zauhar*[,†]

[†]Department of Chemistry & Biochemistry, University of the Sciences, 600 S. 43rd Street, Philadelphia, Pennsylvania 19104, United States

Supporting Information

ABSTRACT: Prostate Cancer (PCa), a leading cause of cancer death worldwide (www.cancer.gov), is a complex malignancy where a spectrum of targets leads to a diversity of PCa forms. A widely pursued therapeutic target is the Androgen Receptor (AR). As a Steroid Hormone Receptor, AR serves as activator of transcription upon binding to androgens and plays a central role in the development of PCa. AR is a structurally flexible protein, and conformational plasticity of residues in the binding-pocket is a key to its ability to accommodate ligands from various chemical classes. Besides direct modulation of AR activity by antagonists, inhibition of cytochrome CYP17 (17α-hydroxylase/17,20-lyase), essential in androgen biosynthesis, has widely been considered an effective strategy against PCa. Interestingly, Handratta et al. (2005) discovered new, potent inhibitors of CYP17 (C-17 steroid derivatives) with pure AR antagonistic properties. Although the antiandrogenic activity of their lead compound (VN/124-1) has been experimentally proven both *in vitro* and *in vivo*, no structural data are currently available to elucidate the molecular determinants responsible for these desirable dual inhibitory properties. We implemented a Structure-based Drug Design (SBDD) approach to generate a valuable hypothesis as to the binding modes of steroidal CYP17 inhibitors/antiandrogens against the AR. To deal with the plasticity of residues buried in the Ligand Binding Domain (LBD), we developed a flexible-receptor Docking protocol based on Induced-Fit (IFD) methodology (www.schrodinger.com/). Our results constitute an ideal starting point for the rational design of next-generation analogues of CYP17 inhibitors/antiandrogens as well as an attractive tool to suggest novel chemical classes of AR antagonists.

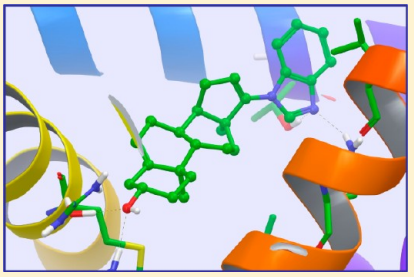

INTRODUCTION

According to the National Cancer Institute, Prostate Cancer (PCa) is a widespread disease in men over age 60 and is actually one of the leading causes of cancer death worldwide, with over 240,000 new cases estimated in the United States alone in 2012 (www.cancer.gov).

Several types of prostate cancers are known; they all develop in the prostate tissues, when normal cells start dividing uncontrollably to form malignant tumors that subsequently spread to other parts of the body, ultimately giving rise to metastases. Many biological targets are held responsible for the development and progression of the various forms of PCa, one and foremost the Androgen Receptor (AR).[1,2] AR is a Nuclear hormone Receptor[3] (NR) comprising functional domains common to other NRs: a variable N-terminal domain (NTD) with regulatory functions; a highly conserved DNA binding domain (DBD) that binds to DNA upon recognizing specific Androgen Response Elements (ARE); a structurally conserved ligand-binding domain (LBD) separated from the DBD by a flexible Hinge Region (HR); and a variable C-terminal domain (CTD).[4,5] Regulation of AR is initiated in the cytoplasm by binding to androgens, thus leading to conformational changes which promote dissociation from molecular chaperones and conversion of inactive AR monomers into active transcription factors. Fully activated ARs translocate to the nuclear compartment where binding to AREs promotes gene transcription.[5]

Androgen-regulated genes are essential to a number of male physiological responses ranging from sexual differentiation and maturation to spermatogenesis.[6] In addition, AR mediates the physiological maintenance of the prostate as well as being implicated in the pathological development and progression of several prostate cancer forms.[7]

While endogenous activation of the AR occurs upon binding of natural steroids (i.e., Testosterone and the more potent 5α-dihydrotestosterone, DHT), many ligands belonging to various chemical classes have also been observed to tightly bind to its flexible LBD, resulting in conformational changes that may produce a variety of modulation effects (ranging from pure agonistic to full or partial antagonistic behaviors). Ligand-dependent conformational changes in AR allow tissue-specific coregulators (coactivators or corepressors) to be recruited before selectively starting the genomic transcriptional machinery, through a regulation mechanism common to other NRs and widely known as Selective Hormone Receptor Modulation (SHRM).[8] In addition, somatic mutations (e.g., Thr877Ala found in LNCaP prostate cancer cells) in the Androgen Receptor Ligand Binding Domain (ARLBD) have been

Received: May 17, 2012
Published: August 27, 2012

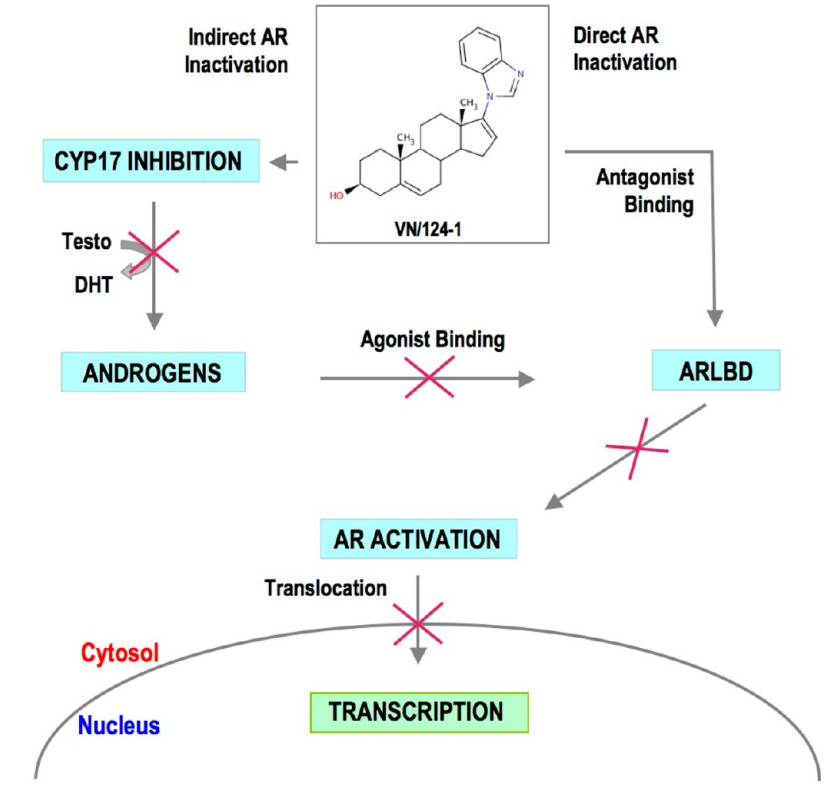

(a)

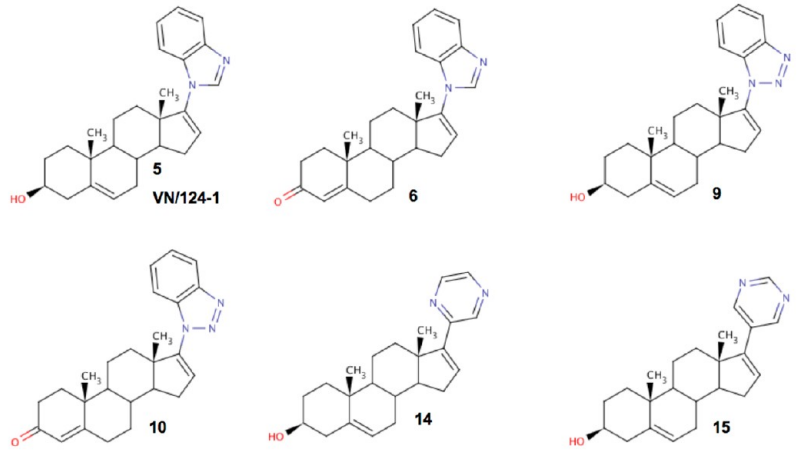

(b)

Figure 1. (a) Direct and indirect AR inactivation properties exerted by VN/124-1[15,22] (also referred to as compound **5** or TOK-001[26]) discovered by Handratta et al. (2005) as novel inhibitor of the cytocrome CYP17,[18] key enzyme in androgen biosynthesis. Remarkably, the authors also demonstrated that this compound shows direct AR inhibitory properties, acting as pure antagonists.[23,24] Thus, in prostate cancer, VN/124-1[22] *dual* inhibition properties act to inhibit AR activity through direct (antagonist) and indirect (CYP17 inhibition) pathways. (b) Chemical structures of steroidal 17-benzimidazole compounds **5** (VN/124-1, TOK-001)[26] and **6**, 17-benzotriazoles **9** and **10**, and 17-diazines **14** and **15** discovered by Handratta et al.[22]

observed in patients with metastatic prostate cancers.[9] These mutations produce single amino-acid substitutions in AR binding pockets and are known for their ability to confer drug resistance to patients being treated with a number of antiandrogens, by changing the activity of these compounds from antagonist (against wild-type ARs) into agonist (against mutated ARs).

What emerges about the conformational properties of AR is a very complex picture: on one side AR may accommodate structurally different ligands sharing common modulating properties (either agonist or antagonist); on the other, the same ligand molecules have been observed to exert opposing responses upon the binding pocket of wild-type versus mutant ARs.[10]

dx.doi.org/10.1021/ci3002342 | J. Chem. Inf. Model. 2012, 52, 2670−2683

Given that the conformational flexibility of the LBD plays such an essential role to AR regulation, understanding the structural determinants responsible for binding interactions and related "induced-fit effects" becomes crucial to Structure-based Drug Design (SBDD). *Per contra*, receptor-based modeling of protein conformational flexibility has long been considered a very demanding task.[11,12] Indeed, while quite a large number of computational studies aimed at designing novel chemical classes of AR ligands have been reported, these typically implement computationally demanding docking solutions in an attempt to incorporate receptor flexibility in drug design.[13,14] While valuable for understanding the details of ligand−receptor interactions, such simulation approaches are less interesting for virtual screening of very large libraries of compounds.

Among several classes of AR modulators, steroidal C-17 derivatives of CYP17 inhibitors/antiandrogens have been recently brought to our attention because of their *dual* inhibitory properties (Figures 1 a and b). Derived from a chemical class originally designed by Njar and colleagues[15−17] as inhibitors of cytocrome CYP17 (17α-hydroxylase/17,20-lyse), a key enzyme in androgen biosynthesis and a well-established target for prostate cancer therapy,[18−21] some of these chemical agents were also found to be active (Table 1)

Table 1. Experimental Activities of 17-Heteroaryl Compounds, Discovered by Handratta et al. (2005), Measured against Androgen Receptor and Cytocrome CYP17[a]

compound no.	AR binding PC3-AR IC_{50} (nM)	AR binding LNCaP IC_{50} (nM)	CYP17 binding IC_{50} (nM)
5	384.00	845.00	300.00
6	242.00	1200.0	915.00
9	nd	nd	1250.0
10	nd	nd	5817.4
14	366.00	nd	3810.0
15	374.00	nd	500.00

[a]The synthesis and biological studies of compounds **5, 6, 9, 10, 14,** and **15** were reported and fully documented elsewhere.[22] As reported by the authors, for AR binding assay, IC_{50} refers to the concentration of compound required for a 50% displacement of [^{3}H]R1881 from the androgen receptor in the PC3-AR and LNCaP cell lines, each in triplicate. For CYP17 inhibition, IC_{50} refers to the concentration of compound required to inhibit the enzyme activity by 50%, each in duplicate. nd = not determined.

against a wild-type AR-expressing cell line (PC-3AR) and a mutant androgen receptor cell line (the androgen-sensitive LNCaP).[22] Remarkably, their lead compound VN/124-1[22] (herein referred to as compound **5**) was also reported to inhibit AR in both *in vitro* and *in vivo* studies[22−24] and achieved an investigational new drug (IND) status to enter phase I/II clinical trials in late 2009 by TOKAI PHARMACEUTICALS under the name of TOK-001.[25,26]

Clearly, the rational design of more potent structural analogs of VN/124-1[22] constitutes a very attractive prospective to the inhibition of both CYP17 and AR, hopefully leading to the discovery of novel classes of therapeutic agents against prostate cancer.

However, only two three-dimensional (3D) structures of CYP17 in presence of small molecule binders[27] (one of them is TOK-001)[26] have been resolved so far (Protein Data Bank),[28] and were published after the work described here was largely completed. In contrast, more than 70 crystal structures of the human AR ligand-binding domain have been solved (Protein Data Bank)[28] in complex with natural androgens, like DHT (e.g., in PDB IDs 2PIP or 2AMA)[29,30] and Testosterone (TES, e.g. in PDB ID 2AM9),[30] and with agonists, such as the chemically modified steroid metribolone (R18, e.g. in PDB ID 1XOW)[31] or the corticosteroid 9α-fluorocortisol (ZK5, PDB ID 1GS4).[32] In addition, structures of the human Androgen Receptor Ligand Binding Domain (hARLBD) have been determined in complex with nonsteroidal ligands (NSL), like the potent Selective Androgen Receptor Modulators (SARMs).[33,34]

To generate a putative binding hypothesis of steroidal CYP17 inhibitors to the human Androgen Receptor we have developed and successfully validated a SBDD approach. Close inspection and comparisons of several AR crystal structures in complex with ligands selected from different chemical classes revealed molecular details of the intrinsic flexibility of the ARLBD, while identifying structural determinants responsible for increasing binding affinities. Our receptor-based modeling was initially based on VN/124-1[22] (compound **5**) docked against the crystal structure of hARLBD in complex with Testosterone (PDB ID 2AM9, Figure 2 a).[30] Conformational changes occurring upon ligand binding have been modeled by the Schrödinger Induced Fit Docking (IFD) methodology.[35−38] Binding mode hypotheses for several C-17 benzimidazole, benzotriazole, and diazine derivatives have been generated against wild-type and mutant ARs, the latter responsible for developing drug-resistant forms of PCa cell lines.

Results demonstrate that IFD can be successfully used to incorporate AR flexibility into drug design. In particular our findings provide strong evidence as to the structural elements necessary to build a useful model of the binding of hARLBD to the class of steroidal CYP17 inhibitors, which have been experimentally proven to serve as AR modulators, some even acting as strong, selective AR antagonists.[22−24] By combining molecular modeling approaches with experimental activities determined against either wild-type AR-expressing cell line (PC-3AR) or PCa resistant Thr877Ala mutant AR (LNCaP cell line),[22] we have validated our model of the flexible receptor. We are confident the model can be effectively applied to the rational design of next-generation analogues of *dual CYP17 inhibitors/antiandrogens* and constitutes an attractive tool to suggest new directions for developing *novel* chemical classes of AR antagonists.

RESULTS AND DISCUSSION

Induced Fit Model of Human ARLBD: Structural Determinants of Molecular Recognition. A variety of natural and synthetic agonists or antagonists have been reported that bind AR over a broad range of affinities, and molecular determinants responsible for their binding have been extensively investigated elsewhere.[30,33,34,39] Nevertheless, it has not been fully clarified how substantially different binding affinities for AR may derive from steroids with highly similar structures, while ligands with relatively low structural similarities could result in comparable binding affinities.[30]

Here we report the analysis of a subset of 29 out of more than 70 publicly available crystal structures of the human ARLBD with a resolution better than 2 Å (query performed on Protein Data Bank[28] on May 1st, 2011). All AR structures (Table 2 and the Supporting Information) were aligned on a common reference 3D-template (2AM9, 1.65-Å resolution),[30] and comparisons between binding modes of steroidal-core

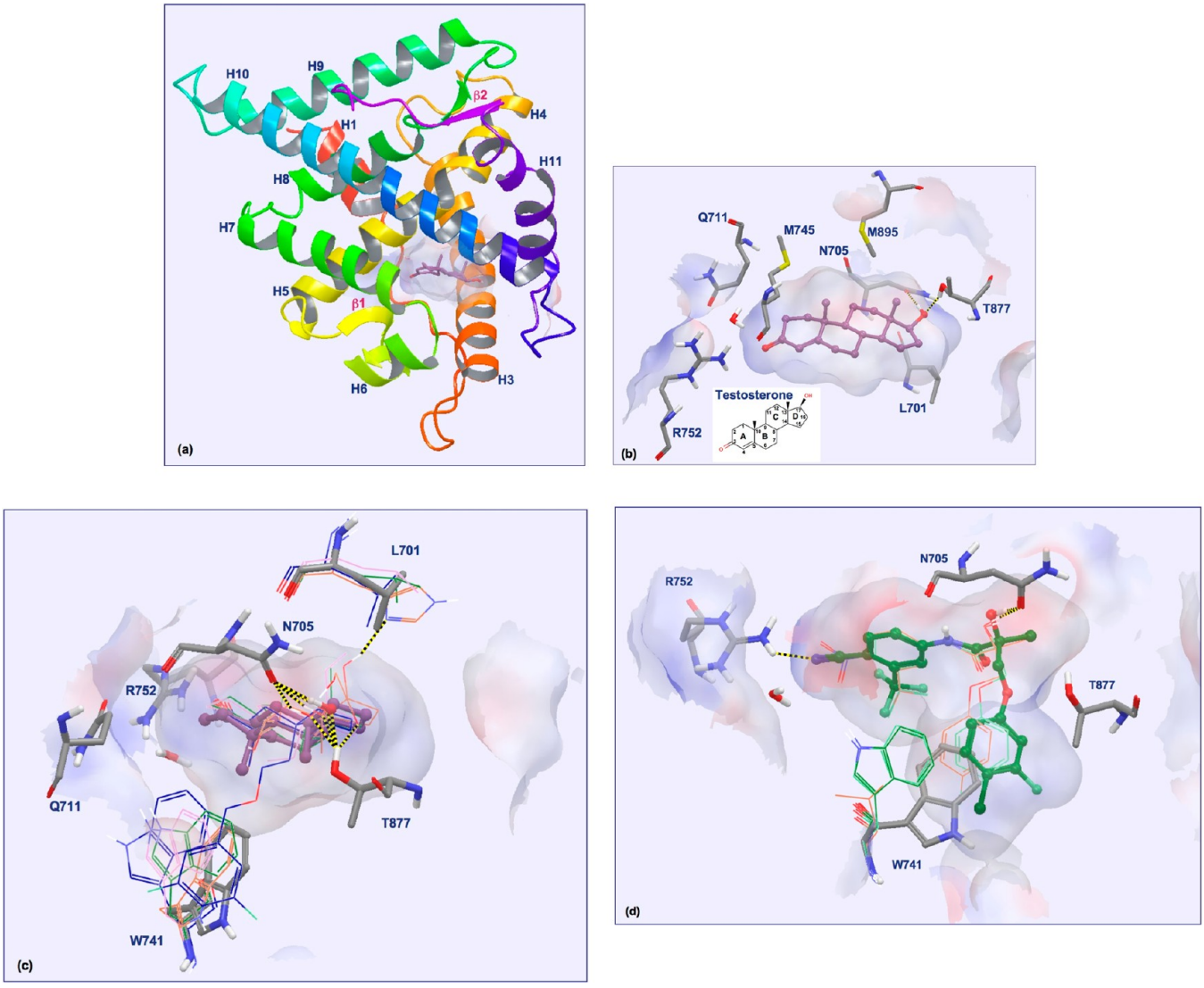

Figure 2. (a) Crystal structure of human Androgen Receptor Ligand Binding Domain (hARLBD) in complex with Testosterone (PDB ID 2AM9).[30] A 12 α-helices sandwich structure is shown to bind a central, mainly hydrophobic cavity where binding-interactions are primarily guided by residues in helices 3, 5, 7, and 11 and in a β-strand located between helices 5 and 6.[4] (b) Selected residues facing the ARLBD are responsible for molecular recognition and binding of the steroid scaffold (in this case Testosterone) via hydrogen bond networks formed with polar atoms located at opposite ends of the bound molecule (polar side 1: Arg752 and Gln711; polar side 2: Asn705 and Thr877). In addition, a number of amino acid residues are involved in hydrophobic interactions via van der Waals contacts (like Met745 and Met895). (c) Superposition of AR crystal structures bound to Testosterone (2AM9[30] is the reference structure; ligand is purple, ball-and-stick rendering; protein is gray-carbons, stick rendering), 9α-fluorocortisol (1GS4[32] orange), tetrahydrogestrinone (2AMB,[30] pink), DHT (1T65,[63] green), and the 5α-dihydrotestosterone-derived molecules bearing a bulky C-18 chain (2PNU,[40] blue). All the ligands except Testosterone are shown in line rendering. The bulky side chain of the aromatic residue Trp741 offers hydrophobic contacts to the C18-methyl groups of DHT and Testosterone, while rotation of its indole-cycle far away from its original position is crucial to enlarge the binding pocket when larger C18-substituents decorate the steroidal C-13 atom. (d) Superposition of AR crystal structures in complex with SARMs revealed ligand-induced mobility of Trp741. Reference receptor structure in gray-carbons (3B5R);[34] Selective Androgen Receptor Modulators (SARMs): light green (2AX7);[33] orange (2AX8);[33] and dark green, ball-and-stick rendering (3B5R).[34]

structures versus nonsteroidal ligands revealed key elements to understand receptor flexibility and elucidate induced fit effects.

The structure of the AR ligand-binding domain comprises a 12 α-helices sandwich that defines a central, mainly hydrophobic cavity where binding-interactions are primarily guided by residues in helices 3, 5, 7, and 11 and in a β-strand located between helices 5 and 6 (Figure 2 a).[4] In all cases of molecules with a steroidal core (18 crystal complexes, 8 different ligand structures; see Table 2 and the Supporting Information for details and references), a few polar residues are essential to fix the scaffold via hydrogen bond networks formed with polar atoms located at opposite ends of the bound molecule. Specifically, at one side, Arg752 and Gln711 side chains interact with the oxygen atom (O3) of the C-3 keto-group of the A-ring, while amino acids Asn705 and Thr877 interact with C-17 substituents located at the other side of the scaffold (D-ring) (Figure 2 b).

In addition, the majority of amino acid residues facing the Ligand Binding Pocket (LBP) are involved in hydrophobic interactions with the steroid nucleus via van der Waals contacts. In particular Met745 interacts with the C19-methyl groups in structures like DHT and Testosterone, while Met895 makes contacts with the C18-methyl group of Testosterone and adopts new conformations when the C-13 carbon atom is

dx.doi.org/10.1021/ci3002342 | J. Chem. Inf. Model. 2012, 52, 2670−2683

Table 2. Crystal Structures of hARLBD Are Listed in Alphabetic Order along with Relative PDB IDs, Ligand Identifiers, ARLBD Mutations, Resolution (Å) Limits, and Ligand Type (Steroid versus Nonsteroid Classification)[a]

PDB ID	ligand identifier	ARLBD mutations	resolution (Å)	ligand-type
1GS4[32]	ZK5	L701H/T877A	1.95	steroid
1T65[63]	DHT		1.66	steroid
1XOW[31]	R18		1.80	steroid
1Z95[43]	198	W741L	1.80	nonsteroid
2AM9[30]	TES		1.64	steroid
2AMA[30]	DHT		1.90	steroid
2AMB[30]	THG		1.75	steroid
2AO6[31]	R18		1.89	steroid
2AX6[33]	HFT	T877A	1.50	nonsteroid
2AX7[33]	FHM	T877A	1.90	nonsteroid
2AX8[33]	FHM	W741L	1.70	nonsteroid
2AX9[33]	BHM		1.65	nonsteroid
2AXA[33]	FHM		1.80	nonsteroid
2OZ7[41]	CA4	T877A	1.80	steroid
2PIP[29]	DHT		1.80	steroid
2PIT[29]	DHT		1.76	steroid
2PIV[29]	DHT		1.95	steroid
2PNU[40]	ENM		1.65	steroid
2Q7I[64]	TES		1.87	steroid
2Q7J[64]	TES		1.90	steroid
2Q7K[64]	TES	H874Y	1.80	steroid
2Q7L[64]	TES	H874Y	1.92	steroid
3B5R[34]	B5R		1.80	nonsteroid
3B65[34]	3B6		1.80	nonsteroid
3B66[34]	B66		1.65	nonsteroid
3B67[34]	B67		1.90	nonsteroid
3B68[34]	B68		1.90	nonsteroid
3L3X[65]	DHT		1.55	steroid
3L3Z[65]	DHT		2.00	steroid

[a]See the Supporting Information for chemical structures and ligand names.

decorated with larger substituents. Also, the bulky side chain of the aromatic residue Trp741 (Figure 2 c) offers hydrophobic contacts to the C18-methyl groups on C-13 of DHT (minimum heavy atom distance 4.08 Å, PDB ID 2PIP[29]), Testosterone (minimum heavy atoms distance 4.15 Å, PDB ID 2AM9[30]), and R18 (minimum heavy atoms distance 4.12 Å, PDB ID 1XOW[31]), and rotation of its indole-cycle far away from its original position is crucial to enlarge the binding pocket when larger substituents decorate the steroidal C-13 atom (C-18 chains), as in the case of Tetrahydrogestrinone (THG) or the agonist 5α-dihydrotestosterone-derived molecules that bear various C-18 chains.[40]

Structural comparison between androgens and VN/124-1 analogs[22] (Figure 1 b) suggest that the introduction of bulky substituents on C-17 of the steroidal D-ring could be a crucial factor in determining molecular recognition. Based on our comparisons of superposed crystal structures, we identified the large, hydrophobic side chain of Leu701 as a leading determinant in establishing induced-fit effects. Leu701 lies in a small, predominantly hydrophobic pocket at the interface between residues Phe697, Leu700, Leu704, Ser778, Met780, Phe876, Leu880, and Val889, and its side chain is located in close contact with the steroidal D-ring in a position that naturally leads it to interact with C17-substituents (Figure 2 b and c).

Indeed, the orientation of the Leu701 side chain can rotate significantly from its original position (when bound to the natural androgens Testosterone and DHT) to occupy a completely new geometry suitable to make room for accommodating bulkier substituents, like the ethyl group at position 17α in the THG structure. We measured the flexibility of the Leu701 side chain, defined as the distance between the two γ-carbon atoms taken from the crystal structures in complex with Testosterone (PDB ID 2AM9)[30] and the steroidal antiandrogen cyproterone acetate (CA4, PDB ID 2OZ7),[41] and find a range of motion of 3.4 Å. Concerning the second structure, it has been observed elsewhere that the dramatic movement of the Leu701 side chain results in the expansion of the AR binding cavity, which becomes suitable for accommodating the bulky 17α-acetate group of CA4.[41] Experimental mutagenesis studies investigated the impact of several Leu701 mutations on AR cell lines and indicated that substitutions at this position strongly affect AR ligand responsiveness.[42]

Furthermore, our analysis also aimed to get a better picture of the structural basis for nonsteroidal ligands (NSL) recognition. Our selection of crystal structures included 11 androgen receptors in complex with either antagonists (bicalutamide and hydroxyflutamide, PDB IDs 1Z95[43] and 2AX6,[33] respectively) or with tissue selective agonists, namely the structurally similar Selective Androgen Receptor Modulators (SARMS, PDB IDs 2AX7,[33] 2AX8,[33] 2AX9,[33] 2AXA,[33] 3B5R,[34] 3B65,[34] 3B66,[34] 3B67[34] and 3B68;[34] Table 2 and the Supporting Information). Again, binding modes are primarily dictated by hydrogen bonds with the polar residues Arg752 and Gln711, but in the case of NSLs, the second polar attachment (Asn705 and Thr877), typical of steroid molecules, is missing (Figure 2 d). Here, the bound ligands engage in additional hydrogen bonds as exhibited by the B-ring *para*-substituted analogs of the nonsteroidal antagonist R-bicalutamide (PDB ID 1Z95,[43] Table 2 and the Supporting Information). On the other hand, pi-stacking interactions are possible between the Fluorobenzene moiety of the nonsteroidal agonist S-1 and the indole-ring of Trp741 (PDB IDs 2AX7[33] and 2AX9,[33] Table 2 and the Supporting Information), providing an additional favorable interaction. Superposition of AR crystal structures in complex with several SARMs (Figure 2 d) shows how ligand-induced mobility of Trp741 also affects the positions of Thr877 and Met895 and demonstrates, once more, that these changes are necessary to accommodate diverse ligands within the binding cavity (Figure 2 c).

Lastly, AR structural analysis also brought to our attention the presence of a water molecule always located at an identical position in the ligand-binding site (Temperature Factor of 21.07 Å^2 in PDB ID 2AM9[30]). In every crystal structure analyzed, a conserved water molecule is found in precisely the same position, in close contact with polar residues Arg752 and Gln711, and is likely to participate in hydrogen-bond interactions with bound ligands (Figure 2 a to c).

In summary, our definition of the Induced Fit Model for AR binding is founded on careful comparisons of crystal structures of hARLBD in complex with diverse ligands. While polar amino acids, aided by water molecules, firmly tether both steroidal and NS cores at distal, polar extremities of the LBP (limited to Arg752 and Gln711 in the NS case), hydrophobic interactions are also required. The intrinsic nonspecificity of the hydro-

dx.doi.org/10.1021/ci3002342 | J. Chem. Inf. Model. 2012, 52, 2670−2683

phobic side chains of a number of amino acid residues facing the LBP in combination with their flexibility may explain the ability of the AR binding cavity to accommodate a variety of structurally distinct compounds, as also observed by other authors.[30] These mobile residues constitute the main components of the induced fit model on which we based our docking simulations.

Induced Fit Docking. Protein flexibility plays an important role in determining receptor/ligand recognition. While critical to understanding receptor−ligand interactions, it is nontrivial to model these effects in the protein active site. Indeed, most of the currently available docking tools allow only ligands, and not protein residues, to adopt multiple conformations, often drastically reducing the degrees of freedom available to the system.

To deal with the native mobility of key residues buried in the AR binding pocket, we implemented a flexible receptor docking protocol using the Induced-Fit tool,[35] distributed by Schrödinger.[36−38] Induced Fit Docking (IFD) is a novel procedure introduced by Sherman et al.,[36] which accounts for protein flexibility by combining the Glide[44−47] algorithm for docking against a fixed protein structure with the Prime[48−50] methodology for predicting alternate conformations of the protein active site. The central idea is that for a given ligand, the receptor is 'induced' to adopt a suitable binding conformation, which is likely to obey the law of structural complementarity between ligand and receptor.

The IFD procedure works in four phases, which are repeated if the first output structures are given similar scores, in order to enhance the accuracy of the protocol.[36] The first stage consists of docking against a rigid receptor structure with the aim of generating an ensemble of initial docked poses of the ligand to be refined in subsequent steps. To account for receptor flexibility, two strategies are implemented in this stage: the first refers to the use of a softened-potential, where van der Waals radii of ligand and receptor atoms are scaled by 50 to 70% to significantly reduce steric clashes. In addition, side chains of selected residues, which are believed to potentially impede ligand access to the binding site, are replaced *ad interim* with smaller alanine side chains.

This is followed by a structure prediction stage, which uses the Refinement module of the Prime program[48] to sample receptor conformations for any ligand poses generated in step one. Here, *ad interim* alanine residues are replaced by the original amino acids. Side-chain predictions/energy minimizations are also executed, and finally a set of optimized receptor conformations, so-called "induced-fit conformations", is generated.

The third step consists of using Glide to redock ligands against selected low-energy induced-fit receptors that are within 30 kcal/mol of the lowest energy structure. Finally, during the fourth step, best binding modes are ranked and selected according to a scoring function described by Sherman et al.,[36] which combines the Prime Energy and the GlideScore, according to the following equation

$$IFD\ Score\ (kcal/mol) = GlideScore + 0.05\ Prime\ Energy$$

(See ref 36.) Here the GlideScore is the protein/ligand interaction energy as computed by the docking tool, and the Prime Energy is the total energy of the protein ligand system found using the OPLS force field[51,52] and an implicit solvent model (surface Generalized Born).[53,54]

Our IFD protocol was developed with the aim of incorporating the conformational plasticity of the AR binding pocket into a molecular docking procedure for receptor-based drug design. As a challenging case study, we chose to generate binding hypotheses for the steroidal CYP17-inhibitors/AR-antagonists to the human ARLBD, thus providing a rational model to experimental results generated by others.[22] The receptor model is based on the very high-resolution (1.65 Å) crystal structure of AR in complex with Testosterone (PDB ID 2AM9,[30] Table 2 and the Supporting Information). The lead compound, VN/124-1,[22] and relative analogs, consist of steroidal C-17 benzimidazole (**5** and **6**), benzotriazole (**9** and **10**), and diazine (**14** and **15**) derivatives (Figure 1 b).[22] The presence of bulky groups at the C-17 position of the steroidal core explains our decision to consider Leu701 as the residue that likely undergoes the largest induced-fit effects. In addition, given the high flexibility highlighted during the structural analysis of many ARs bound to diverse ligands, the indole side chain of Trp741 was also considered critical to accommodate ligands over the course of IFD runs involving both nonsteroidal ligands (SARMs) and steroidal compounds that bear unwieldy C-13 substituents. Thus, Leu701 and Trp741 were selected during the initial Glide docking step to be temporarily removed and replaced by alanine residues.

During the Prime Refinement stage of the IFD protocol, temporary alanine residues were restored back to their original type, and a shell comprising all residues having at least one atom within 5 Å of the ligand was submitted to Prime for side chain predictions and Molecular Mechanics energy minimization (MM OPLS2005 force filed) steps to generate the final ensemble of induced-fit AR conformations.

Redocking Ligands from Crystal-Structures: A Validation Step. In the course of the development of an induced-fit docking model, it is crucial to assess the ability of the method to accurately accommodate a variety of ligands by generating side-chains conformations of flexible residues that match experiment.

Therefore, we initially tested our IFD methodology for its ability to redock ligands from available crystal structures, and we took the results as an indication of IFD accuracy in predicting binding modes of VN/124-1[22] and analogs for which no experimental data are available.

The crystal structures of AR in complex with different ligands which we have used as our validation set are reported in Tables 2 and 3 and the Supporting Information. As described above, the IFD receptor was the high-resolution AR structure in complex with Testosterone (see Materials and Methods section for details) where Leu701 and Trp741 side chains were considered critical residues to accommodate ligands within the binding site of AR and were modeled flexibly by means of temporarily mutating them to Alanine resides in the initial Glide docking step. Again, all residues of the binding site within 5 Å of any docked ligands were selected for the refinement stage of minimization (MM OPLS2005 force-field).

Best poses generated by IFD for all the ligands in the validation set are reported in Figure 3 (a) to (g). Docking scores, listed in Table 3 along with a heavy-atom root-mean-square deviation (rmsd, Å) of predicted ligands from their respective crystal-structure geometries, clearly validate our IFD approach. In addition, for any complex of the validation set, side-chain positions of all residues held responsible for specific binding interactions were found to match experiment.

Table 3. IFD Results for the Validation Set[a]

ligand	glide evdw kcal/mol	glide ecoul kcal/mol	XP Gscore kcal/mol	XP Hbond kcal/mol	IFD Score kcal/mol	ligand rmsd (Å)
DHT	−48.59	−10.43	−13.43	−1.977	−485.5	0.001
TES	−48.53	−10.84	−13.14	−1.855	−485.6	0.002
THG	−45.74	−10.09	−13.31	−1.988	−484.6	0.000
R18	−49.16	−11.04	−12.89	−1.994	−485.1	0.015
CA4*	−63.71	−3.970	−12.71	−1.345	−485.4	0.006
ZK5*	−47.32	−9.950	−13.49	−2.197	−482.3	0.004
ENM	−53.33	−10.26	−15.75	−1.330	−489.9	0.043

[a]RMSD (Å) have been calculated for redocked ligands and compared to the original crystal structures. 5-alpha-Dihydrotestosterone (DHT) was extracted from 2AMA,[30] Testosterone (TES) from 2AM9,[30] tetrahydrogenstrinone (THG) from 2AMB,[30] methyltrienolone (R18) from 1XOW,[31] cyproterone acetate (CA4) from 2OZ7,[41] 9-alpha-fluorocortisol (ZK5) from 1GS4,[32] and(5S,8R,9S,10S,13R,14S,17S)-13-{2-[(3,5-difluorobenzyl)oxy]ethyl}-17-hydroxy-10-methylhexadeca-hydro-3H-cyclopenta[a]phenanthren-3-one, EM5744 (ENM) from 2PNU.[40] Ligands extracted from Mutant Androgen Receptor crystal structures are marked with (*).

For all the androgens considered, binding modes predicted by redocking were very close to the experimental structures; the predictive accuracy, measured in terms of rmsd of the best docking mode relative to the crystallographic orientation, ranged from 0 to 0.043 Å. Even in the case of androgens decorated by long and flexible chains, as in the case of the steroidal ligand ENM (PDB ID 2PNU),[40] the rmsd is still very low (0.043 Å, Figure 3). IFD results are even more impressive in the case of the antiandrogen cyproterone acetate (CA4, PDB ID 2OZ7)[41] and of the agonist 9α-fluorocortisol (ZK5, PDB ID 1GS4).[32] Indeed, both crystallographic complexes show substitutions in one or more amino acids at the binding cavity. Remarkably, the IFD model generates reliable binding modes, which fully reproduce crystallographic orientations.

Binding Mode of Steroidal CYP17 Inhibitors/Antiandrogens to the hARLBD. Binding mode hypothesis for the lead compound, VN/124-1[22] (compound **5**), to the hARLBD is shown in Figure 4 (a), with Glide-XP and the IFD scores of −15.33 kcal/mol and −486.6 kcal/mol, respectively (Table 4). As expected considering the structural similarity of this chemical compound to natural androgens, the orientation of the steroidal nucleus within the AR binding pocket is highly conserved. At one polar side of the steroid moiety of compound **5**,[22] the C-3 keto-oxygen of the A-ring (which is always present in androgens that bind the AR with high affinity) is replaced by a hydroxyl group. In this case, Gln711 and Arg752 (hydrogen-heavy atom distance 2.09 and 2.02 Å, respectively) play a central role by forming a hydrogen bond network with one water molecule, which donates a hydrogen atom to the C-3 hydroxyl oxygen of **5**. The ε-NH2 group of Gln711 provides one additional hydrogen atom, giving rise to a network of three hydrogen bonds. This interaction is strengthened by the proximity of the backbone carbonyl-oxygen of Phe764, likely to accept the hydrogen donated by the C-3 hydroxyl group of **5** (the distance between the two heavy atoms is 3.2 Å). At the end of the steroidal nucleus (D-ring) distal to the hydroxyl, the docking pose of **5** suggests the presence of hydrogen bonding between the N atom of the C-17 benzimidazole-substituent and the side chains of Thr877 and Asn705; similar interactions are observed in experimental complexes including potent androgens (Testosterone, DHT, and THG), and indeed the conformations of these side chains match the experimental structures. In contrast, the flexible side chain of Leu701 moves to accommodate the bulky benzimidazole-group of **5** within a small pocket defined by residues Phe697, Leu704, Ser778, Met780, Phe876, Leu880, and Val889, and this leads to a gain in the number of hydrophobic interactions that further stabilize the complex.

Our IFD simulations generated alternative binding modes for compound **5**, which we have examined carefully. In all these cases, the steroid-core was firmly tethered by the same polar attachments at distal positions, resulting in a very similar orientation of the scaffold within the binding cavity. The important interactions established by the C-17 benzimidazole-substituent (of the steroid D-ring) with Thr877 and Asn705 were maintained in the various docking modes, even though the benzimidazole-ring may have shifted slightly. In any event, we have considered these alternative solutions proposed by IFD to better describe the recognition pattern of the C-3 hydroxyl substituent (of the A-ring) of **5**. In particular, we examined an alternative binding-mode (**5** alt-BMode in Table 4, XP-Glide score −13.10 kcal/mol; IFD score −483.0 kcal/mol) of **5** where the C-3 hydroxyl oxygen of the A-ring serves as hydrogen bond acceptor from the NH2 group of Arg752 and in turn donates a H-atom to the backbone carbonyl-oxygen of Met745 (Figure 4 b). The hydrogen atoms of the water molecule previously engaged in a direct interaction with the C-3 hydroxyl oxygen of **5** here adopt a different orientation and are involved in weaker interactions. In this IFD complex, the Gln711 side chain moves from its original location to adopt a new orientation where its NH2 group is likely too far from the C-3 hydroxyl-group of **5** to effectively contribute to the molecular recognition.

We made use of several criteria to discard the latter binding mode in favor of the hypothesis that we described earlier and that, according to our investigations, best represents the specific recognition of compound **5** by the hARLBD. First, we favor the original modality of binding based on visual inspections and docking scores. In our favored binding hypothesis, an intricate network of hydrogen bonds (Asn752, Gln711, Phe764, and one water molecule, XP-Glide score −15.33 kcal/mol; IFD score −486.6 kcal/mol) provides a higher count of favorable interactions compared to the second case (Asn752 and Met745, XP-Glide score −13.10 kcal/mol; IFD score −483.0 kcal/mol), where some molecular counterparts are no longer available. Second, in support of our choice of the first binding mode, we note that it is reproducible within the chemical class of interest, in particular for the predicted complex involving compound **9**[22] (XP-Glide score −14.57 kcal/mol; IFD score −487.0 kcal/mol) (Figure 4 c), and also for other compounds with different scaffolds but similar substitution patterns currently under investigation (data not shown).

Finally, we further investigated the orientation of the amidic-group of the Gln711 side chain with respect to the C-3 hydroxyl group of **5** (and **9**). Starting from the first binding mode herein described for compound **5** (Glide-XP score of −15.33 kcal/mol; −486.6 kcal/mol), we manually changed the orientation of the Gln711 side chain before refining the complex by energy minimization (MM OPLS2005 force-field). Similar to what has been observed by others in the analysis of the crystal structure of hARLBD in complex with Testosterone (PDB ID 2AM9),[30] we obtained an alternative conformation of Gln711 that is flipped with respect to its original orientation (Figure 4 d). As a result of this change of conformation, the

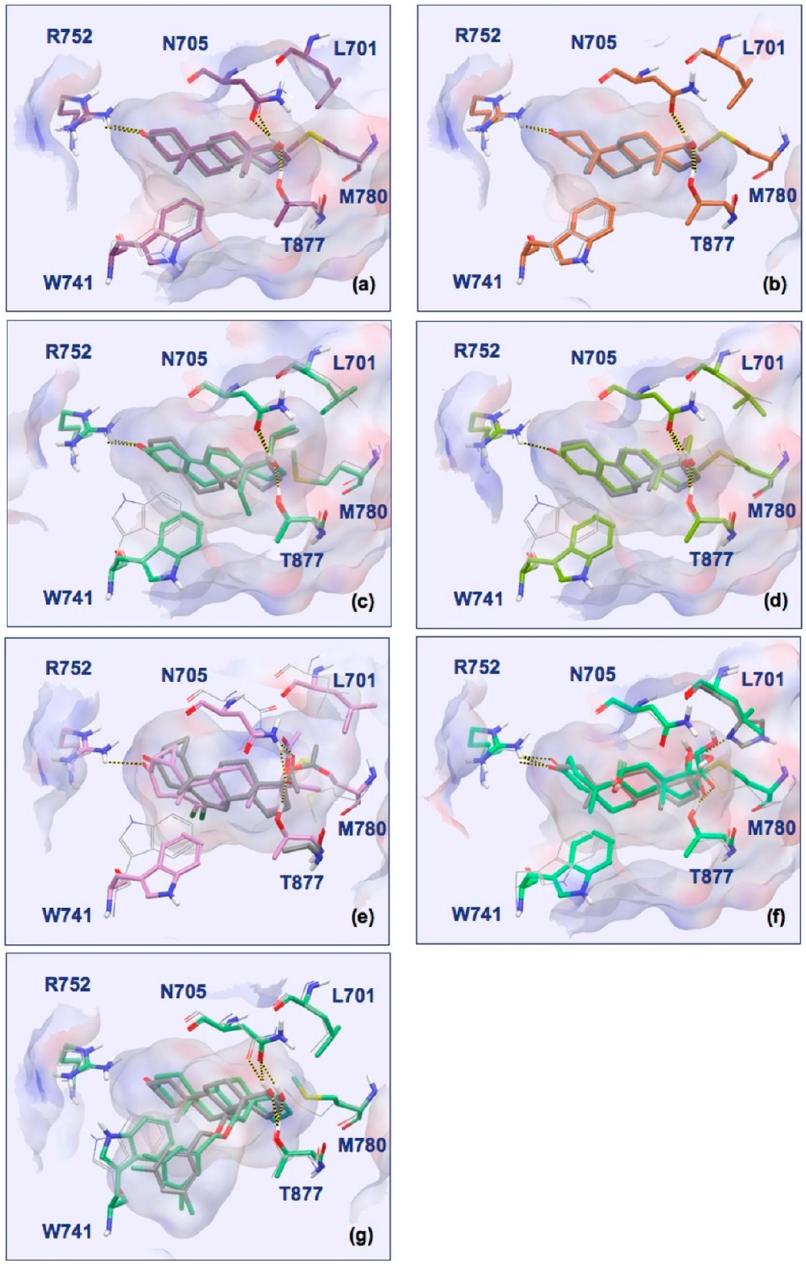

Figure 3. Induced Fit Docking (IFD)[35−37] results for the validation set. In all pictures, binding modes predicted by IFD for any ligands in the set are reported in stick mode with different-color carbons; docking modes are superposed to the relative crystallographic reference structures, reported in gray-carbons (stick rendering the native ligand; line rendering the native receptor) for any binding complexes proposed, IFD yielded very low rmsd to the crystallographic reference ligand (2AM9).[30] (a) 5-alpha-dihydrotestosterone (DHT); (b) Testosterone (TES); (c) tetrahydrogestrinone (THG), (d) methyltrienolone (R18); (e) cyproterone acetate (CA4); (f) 9-alpha-fluorocortisol (ZK5); (g) (5S,8R,9S,10S,13R,14S,17S)-13-{2-[(3,5-difluorobenzyl)oxy]ethyl}-17-hydroxy-10-methylhexadecahydro-3H-cyclopenta[a]phenanthren-3-one (ENM).

hydrogen bonding properties of Gln711 side chain are altered, from Gln711 acting as a hydrogen bond donor (through ε-NH2) to serving as an acceptor (through Oε1) of the H-atom donated by the C-3 hydroxyl group of **5**.

To further investigate the role of the C-3 hydroxyl substituent of the A-ring in the binding mode of compound **5** (as opposed to the more common keto-oxygen found in Testosterone and other steroid ligands), we have also included in our analysis a comparison to the crystal structure of the Estrogen Receptor binding pocket in complex with the agonist 1β-estradiol (hERa-LBD, PDB ID: 1ERE),[55] which bears the same chemical feature of compound **5**. Structural comparison of the newly generated AR-complex with the Estrogen Receptor binding pocket in complex with 1β-estradiol reveals highly similar recognition patterns (Figure 5), with the exception of Gln711 that is replaced by Glu353 in ER. In both cases, the hydroxyl group donates a hydrogen bond to a carbonyl group on the side chain of a binding pocket residue (AR Gln711 amide carbonyl group or ER Glu353 carboxylic acid group), while the hydroxyl oxygen is involved in a network of three hydrogen bonds with an arginine side chain (AR Arg752 or ER Arg394) and a water molecule located in similar position of the binding site. We took this structural comparison as a strong evidence to further confirm our first binding hypothesis (regardless the orientation adopted by Gln711).

dx.doi.org/10.1021/ci3002342 | J. Chem. Inf. Model. 2012, 52, 2670−2683

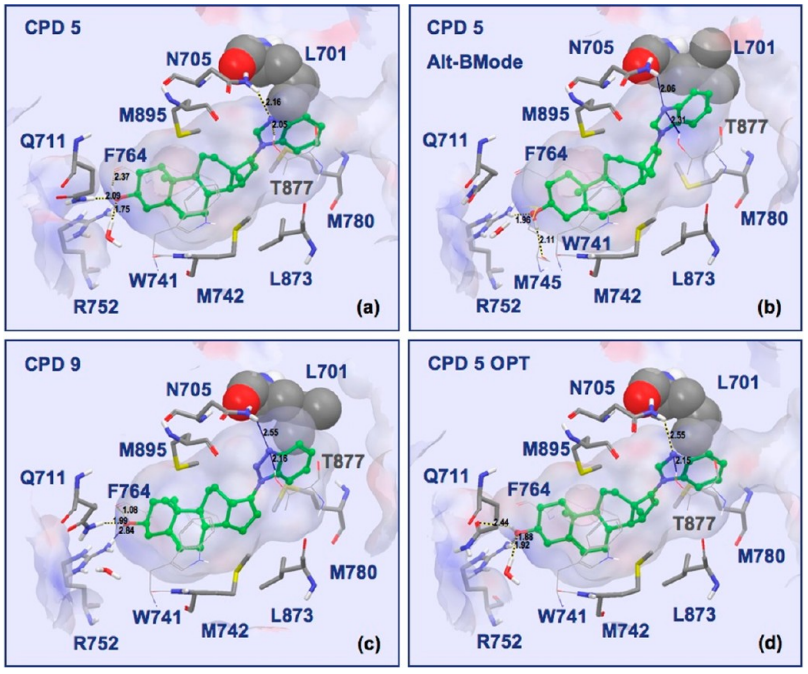

Figure 4. (a) Best docking complex proposed by IFD[35−37] for the lead-compound VN/124-1[22,26] (compound **5**). (b) Alternative binding mode for **5**. (c) Best docking complex proposed by IFD for compound **9**. (d) Minimization (OPLS 2005) of the best docking complex generated for compound **5** after optimization of Gln711 orientation (CPD 5 OPT). In all cases, ligands are shown with green carbons, ball-and-stick rendering; residues facing the binding pocket are shown with gray carbons, line or stick rendering; L701 is shown in space-filling rendering.

Table 4. IFD Results for Compound 5 (VN/124-1)[22] and Analogs against a Flexible Receptor Model of the hARLBD (2AM9[30] As Receptor Template)[a]

CPD#	glide evdw kcal/mol	glide ecoul kcal/mol	XP GScore kcal/mol	XP HBond kcal/mol	IFD score kcal/mol
5	−52.95	−15.47	−15.33	−2.498	−486.6
5 alt-BMode	−53.69	−7.491	−13.10	−1.852	−483.0
9	−53.71	−7.855	−14.57	−2.145	−487.0
6	−57.95	−5.710	−14.35	−1.292	−487.2
10	−59.74	1.307	−12.25	0.000	−484.5
14	−49.99	−7.213	−14.66	−1.358	−485.3
15	−55.44	−5.888	−13.96	−1.024	−491.7
5 T877A*	−54.58	−3.260	−12.12	−1.344	−473.3
6 T877A*	−50.24	−2.377	−10.88	−0.784	−471.7

[a]IFD results obtained using a Mutant Androgen Receptor structure (2AX6[33] as receptor template) are marked with (*).

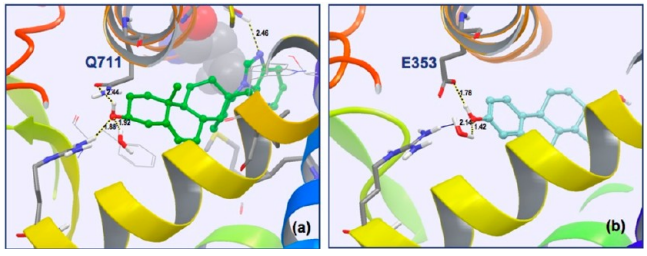

Figure 5. Comparison of (a) the optimized binding-mode predicted for (VN/124-1)[22,26] compound **5** within hARLBD and (b) the crystal structure of the human Estrogen Receptor Ligand Binding Domain (hERa-LBD) complexed with 17β-estradiol (PDB ID: 1ERE[55]) reveals highly similar recognition patterns. Glu353 in ER replaces amino acid Gln711 in AR.

Compound **6**[22] is the C-3 keto-analog of **5**. The binding mode proposed for this compound (Figure 6 a) has a score of −14.35 kcal/mol (XP-Glide; IFD score −487.2 kcal/mol, Table 4). Both the steroid scaffold and the C-17 end of structures **5** and **6** are almost perfectly superimposable (with the exception of the A- and B-rings that adopt slightly different conformations imposed by shifting the C4−C5 unsaturation of **6** to C5−C6 in **5**). As a consequence, binding interactions at the C-3 polar side are similar to what was observed in the case of Testosterone, DHT, and the other androgens with the same structural feature: Arg752 provides an H atom to the acceptor keto-oxygen of **6**, aided by the presence of a water molecule. The substitution of the keto group in **6** leads to a loss of hydrogen bonding strength compared to compound **5**, as evidenced by the 'XP HBond contribution' terms of −1.292 kcal/mol and −2.498 kcal/mol for **6** and **5**, respectively. However, overall stronger van der Waals interactions (as predicted by the Prime and Glide terms: 'Prime vdw' of −1390 kcal/mol for compound **6**, −1318 kcal/mol for compound **5**; in Table 4 'Glide evdw' −57.95, −52.95 kcal/mol for **6** and **5**, respectively) contribute to a global IFD score that, in agreement with experimental inhibitory concentrations (PC-3AR: 242 nM IC_{50} for **6** and 384 nM IC_{50} for **5**), favors **6** over **5**.

Similar binding modes have also been generated for compounds **9** (Figure 4 c, XP-Glide score −14.57 kcal/mol; IFD score −487.0 kcal/mol, Table 4) and **10**[22] (Figure 6 b, XP-Glide score −12.25 kcal/mol; IFD score −484.5 kcal/mol, Table 4), the benzotriazole derivatives of compounds **5** and **6**, respectively. Comparisons of binding modes of **9** versus **5** and **6** versus **10** revealed almost identical scaffold orientations and little or no differences in the conformations adopted by the respective heterocyclic rings.

Lastly, we have also generated binding mode hypotheses for two C-17 diazine derivatives of **5**, compounds **14**[22] (XP-Glide score −14.66 kcal/mol; IFD score −485.3 kcal/mol, Table 4),

dx.doi.org/10.1021/ci3002342 | J. Chem. Inf. Model. 2012, 52, 2670−2683

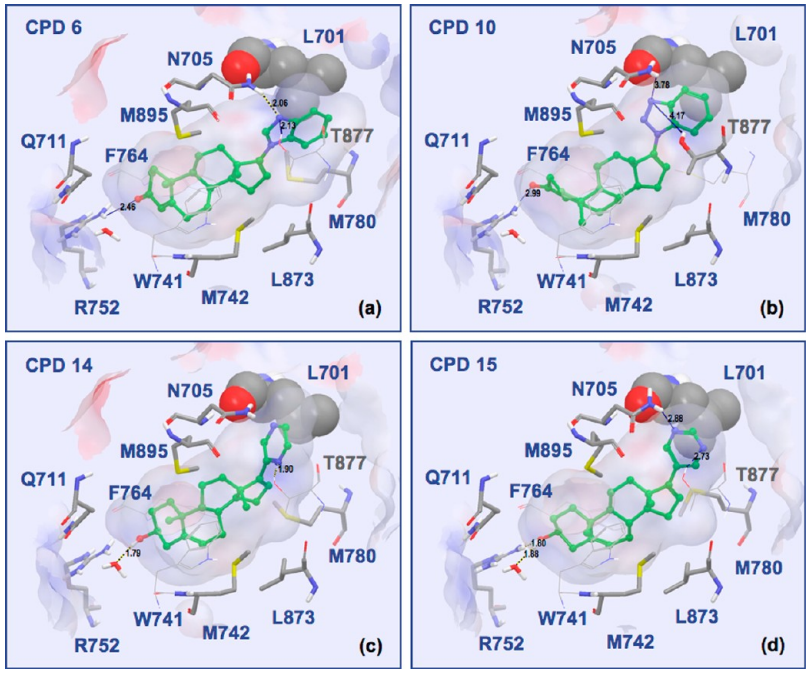

Figure 6. Best docking-complexes generated by IFD for compound **5** (VN/124-1)[22,26] analogues. (a) Compound **6**. (b) Compound **10**. (c) Compound **14**. (d) Compound **15**. In all cases, ligands are shown with green carbons, ball-and-stick rendering; residues facing the binding pocket are shown with gray carbons, line or stick rendering; Leu701 is shown in space-filling rendering.

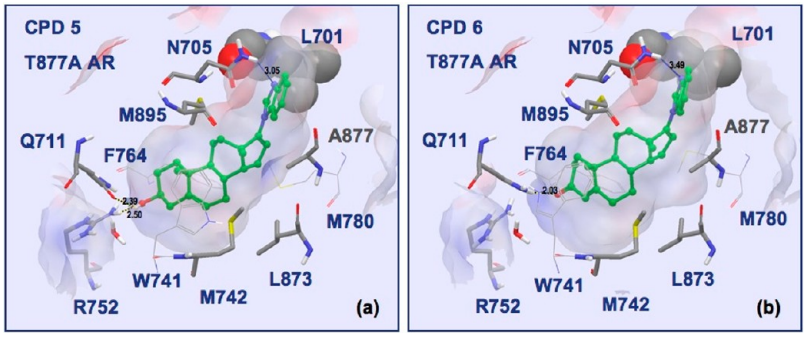

Figure 7. Best docking-complexes generated by IFD for compound **5** (VN/124-1)[22] (a) and compound **6**[22] (b) against the LNCaP mutant AR (Thr877Ala). In both cases, ligands are shown with green carbons, ball-and-stick rendering; residues facing the binding pocket are shown with gray carbons, line or stick rendering; L701 is shown in space-filling rendering.

and **15**[22] (XP-Glide score −13.96 kcal/mol; IFD score −491.7 kcal/mol, Table 4), which show experimental activity data not dissimilar to that of the lead-compound (Figures 6 c and d, respectively). In both compounds, the six-membered rings are embedded in the small, mostly hydrophobic pocket defined by residues Met745, Leu873, Phe876, Met780, Met742, Thr877, and Phe891 and establish two interactions with the polar side chains of Thr877 and Leu705, giving rise to very similar XP-docking and IFD scores.

Structure–Function Analysis of Compounds 5 and 6 Binding Modes against Wild-type versus Mutated AR Structures. When compounds **5** and **6** were tested in AR Binding Assay for their ability to displace the labeled androgen ([^{3}H]-R1881) in the androgen-sensitive LNCaP prostate cancer cell line, Handratta et al.[22] have observed a significant potency reduction for both compounds (Table 1). Interestingly, LNCaP is an androgen-sensitive prostate cancer cell line that contains the functional mutation Thr877Ala in its AR ligand-binding domain.[9] Experimental mutagenesis studies combined with crystallographic analysis demonstrated that Thr877Ala substitution has a strong impact on the size, shape, and properties of AR binding cavity.[42] This structural change is reflected not only in dramatic effects on binding affinities of agonists and antagonists of AR but also in altering their androgenic properties. It is well documented that, in the presence of somatic mutations of AR like Thr877Ala, potent *antagonists* of the wild-type AR, used to treat advanced PCa forms, can behave as functional *agonists*, and this mechanism is responsible for the development of many treatment resistant forms of prostate cancers.

As experimentally demonstrated by Handratta et al.[22] substitution of the polar Thr877 by the smaller, hydrophobic alanine significantly decreases the affinity of compounds **5** (845 nM) and **6** (1200 nM) for AR (more than 2-fold in the case of compound **5** and almost 5-fold for compound **6**, Table 1), confirming the key, structural role of this amino acid in determining molecular recognition. However, although severely affecting their potencies, this mutation seems not capable of totally compromising the antiandrogenic properties of these compounds that were found to serve as pure antagonists (low

dx.doi.org/10.1021/ci3002342 | J. Chem. Inf. Model. 2012, 52, 2670−2683

μM range) when tested for their ability to inhibit the growth of DHT stimulated LNCaP and LAPC4 cells lines.[22]

We chose the high-resolution crystal structure of Thr877Ala mutant AR (which corresponds to the functional mutation found in LNCaP cells) in complex with hydroxyflutamide (1.5 Å resolution, PDB ID 2AX6),[33] and we computationally tested compounds **5** and **6** against our new model system by IFD (see Materials and Methods for details).

Docking poses of compounds **5** and **6** against the Thr877Ala mutant ARLBD are reported in Figures 7 (a) and (b), respectively. As expected, the core scaffold of both compounds assumes the orientations common to all the steroids, albeit with significant deviations from the geometries of binding observed in the case of the wild-type AR structure.

In fact, the Thr877Ala mutation, while increasing the hydrophobic character of the binding pocket, also results in loss of one of the two key interactions provided by polar residues (Thr877 and Asn705) to C-17 substituents, significantly worsening the docking scores. As a consequence, the benzimidazole-rings of both **5** and **6** adopt different orientations to fit within the new cavity. A slight displacement of the core scaffold is also observed in the case of compound **6**, further penalizing the relative docking scores (Table 4).

As shown in Table 4, experimental binding affinities measured for **5** and **6** to the mutant AR are correctly ranked by both Glide-XP and IFD scores (compound **5**: PC-3AR 384 nM IC_{50}, Glide-XP score −15.33 kcal/mol, IFD score −486.6 kcal/mol; LNCaP 845 nM IC_{50}, Glide-XP score −12.12 kcal/mol, IFD score −473.3 kcal.mol). Compound **6**: PC-3AR 242 nM IC_{50}, Glide-XP score −14.35 kcal/mol, IFD score −487.2 kcal/mol; LNCaP 1200 nM IC_{50}, Glide-XP score −10.88 kcal/mol, IFD score −471.7 kcal.mol). Interestingly, the greater effect on **6** exerted by the substitution of Thr877 for Ala on experimental binding affinities (LNCaP cells: 1200 nM IC_{50} for **6** and 845 nM IC_{50} for **5**) is in agreement with the hydrogen bonding contributions computationally predicted for the two ligands (XP HBond for compound **6**: −0.784 kcal/mol; XP HBond for compound **5**: −1.344 kcal/mol).

The only structural difference between compounds **5** and **6** is the presence of C-3 hydroxyl-oxygen on the A ring on compound **5**, which is substituted by a keto-oxygen moiety in compound **6**. The different arrangement of the hydrogen-bonding network established among the ligands and residues Arg752 and Gln711 (mediated by the presence of a structural water molecule) results in weakening this polar interaction, due to exclusion of Gln711 from compound **6** binding mode. On the other hand, low experimental IC_{50} of compound **6** (242 nM) against the native receptor is computationally explained by the strong van der Waals contribution estimated by IFD calculations (Prime vdw' of −1390 kcal/mol; Glide evdw' −57.95 kcal/mol in Table 4), which significantly stabilizes the docking mode predicted for compound **6**.

Knowing that polar interactions established by C-3 and C-17 atoms and relative substituents provide a significant contribution to the steroid scaffold binding, it follows that loss of the same hydrogen bond interaction (a H-atom donated by Thr877 to the N-atom of identical benzimidazole substituents) exerts a dramatic impact on the binding mode (and affinity) of **6**, as evidenced by comparing hydrogen bond contributions to the wild-type (compound **6**: −1.292 kcal/mol; compound **5**: −2.498 kcal/mol) versus the mutated (compound **6**: −0.784 kcal/mol; compound **5**: −1.334 kcal/mol) AR IDF structures.

Nevertheless, our calculations confirm the experimental result that compound **6**, while losing more hydrogen-bonding stabilization compared to **5**, is nonetheless a stronger binder. This further confirms the role of receptor plasticity in stabilizing ligand complexes in diverse and perhaps unexpected ways and points up the importance of incorporating receptor flexibility in computational studies aimed at predicting and rationalizing binding modes and ranking compounds by expected affinity.

CONCLUSIONS

Androgen Receptor is a well-established drug target for PCa therapy and a variety of drug discovery strategies have been implemented that address this pharmacological protein. Traditionally, the vast majority of efforts in antiandrogens discovery has been directed to design small-molecule antagonists acting by preventing the binding of endogenous androgens to the LBP.

A more recent challenge in AR antagonists design concerns AR peptide inhibitors.[56] Although still in its early stage, this approach is very promising, and many peptides targeting the LBP (or, to a lesser extent, other AR-protein interfaces) are currently under investigation as AR antagonists.

Among the many antiandrogens nowadays available, VN/124-1[22] and analogs are a class of steroidal C-17 derivatives that constitute a promising example of targeted polypharmacology. Acting as inhibitors of human CYP17 enzyme as well as potent antagonists of both wild-type and mutant ARs, VN/124-1[22] analogs meet all the requirements to be considered as *dual inhibitors* and represent a novel opportunity for prostate cancer therapy.

Initially designed as an inhibitor of androgen biosynthesis via inhibition of the CYP17 enzyme (with IC_{50} value of 300 nM), VN/124-1[15,22] was later found to competitively inhibit AR with high efficacy in several prostate cancers models both *in vitro* and *in vivo*.[22−24] On the basis of this and other antitumor efficacy studies,[24] VN/124-1[22] (TOK-001)[26] is currently in further preclinical and clinical development by TOKAI PHARMACEUTICALS.[26] An ARMOR1 (Androgen Receptor Modulation Optimized for Response 1) phase I trial in castration-resistant prostate cancer patients was initiated in 2009 and is currently ongoing.[25]

Although several structures of the AR are available in the Protein Data Bank, none of them is complex with C-17 steroidal analogs of VN/124-1.[22] Therefore, no information is currently available for receptor-based ligand design and optimization.

In our comprehensive study aimed at elucidating the binding mechanism of VN/124-1[22] analogs to the androgen receptor, we generated binding mode hypotheses for these structures to the hARLBD, and we modeled the structural interactions responsible for molecular recognition; moreover, experimental results of others[22] have been rationalized through the models generated. Due to the intrinsic plasticity of residues facing the AR binding cavity, our interaction model was founded on a flexible receptor docking protocol reproducing induced-fit effects. The learning phase was based on a systematic analysis of available crystal structures of the hARLBD bound to different chemical classes of ligands. According to the steroidal nature of VN/124-1[22] analogs, we initially focused our attention on AR in complex with a diverse set of steroids, both natural and synthetically derived. This analysis allowed the identification of key amino-acid side chains responsible for the conformational

changes that occur in the LBP upon binding to steroidal core structures. In addition, the ability of our docking model to reproduce induced-fit effects has been improved by integrating structural information derived from NSLs, experimentally bound to the AR.

Our findings show, *in primis*, that Induced Fit Docking can be can be successfully used to generate binding mode hypotheses of active steroid derivatives, like VN/124[22] analogs, for structure based lead-optimization. In agreement with experimental IC_{50} data against both a wild-type AR-expressing cell line (PC-3AR) and a PCa resistant Thr877Ala mutant AR (LNCaP) cell line, we strongly believe that our approach may be very effective to discover new starting points for the rational design of the next generation of *dual AR-antagonist/CYP17-inhibitors* with desirable anti prostate cancer properties.

In secundis, given its proven ability to reproduce crystallographic binding geometries of a broad range of chemical classes of AR binders as well as to score docked compounds in agreement with IC_{50} data against both wild-type and mutant ARs, we propose our flexible receptor model as an effective tool to screen and prioritize a broad range of completely *novel* chemical scaffolds as well as to study steroid derivatives bearing previously unexplored substituents to the steroidal core structure (data not shown).

MATERIALS AND METHODS

Protein Structures Preparation and Alignment. Crystal structure coordinates of androgen receptor proteins were obtained from the RCSB Protein Data Bank.[28] At the time of writing, the unrestricted query performed on ARLBD provided more than 70 structure hits, which were last reduced to 29 human, high-resolution (less than 2 Å) ARLBD structures (Table 2 and the Supporting Information).

All proteins were aligned using the Protein Structure Alignment module in Prime (version 2.2)[48−50] using the PDB ID 2AM9[30] as common reference 3D-template. Aligned structures were prepared according to the Protein Preparation Wizard available in the Schrödinger Maestro software package (version 9.1)[57] for the platform Linux-x86. Hydrogen atoms were added; all water molecules within 5 Å of the ligand were retained during this phase of the project. Prime[48−50] was used to predict missing side chains in the cases of PDB structures missing side-chain atoms. Appropriate ligand bond-orders and formal-charges were adjusted in Maestro. Lastly, a full minimization of any AR complex was performed using the impref utility, which is run by the Protein Preparation Wizard by using the Impact[58] program to perform restrained optimization of the ligand−receptor complexes and allow structure relaxation. The OPLS2005 force field was used, and a 0.30 Å rmsd atom displacement was set for minimization convergence.

Ligands Preparation. All the compounds were prepared with the dedicated Schrödinger tool LigPrep (version 2.4)[59] with initial 3D geometries either generated from 2D sketches (for the VN/124-1 analogs)[22] or taken from the crystal structure geometries (for the validation set compounds). For each ligand structure, various states in terms of stereochemistry and ring conformations were explored. The tautomeric and ionization states of any compound were assigned using Epik (version 2.1)[60−62] at physiological pH. All of the resulting compound-states were energy minimized with OPLS 2005 force field before docking calculations.

Induced Fit Docking. All docking calculations were performed using Glide (version 5.6)[44−46] by means of the Induced Fit Docking software tools available in the Schrödinger Suite 2010.[35]

Glide Grid Setup: Receptor grids were centered at the centroid of the selected crystal ligands. No receptor H-bond or metal constraint atoms were selected.

Step-specific Options: Step (1) Initial Glide Docking. During the "Initial Glide docking" step of the IFD procedure, constrained minimizations of the AR structures were performed with an rmsd cutoff of 0.18 Å (Prime version 2.2, Protein Preparation module).[48] Then, Leu701 of the AR crystal structures in complex with Testosterone (PDB ID 2AM9)[30] or hydroxyflutamide (PDB ID 2AX6)[33] were treated flexibly by temporarily replacing their side chains with the methyl-group of alanine. In addition, also Trp741 was flexibly treated (by replacing its indole side-chain with alanine) over the course of IFD runs involving steroid ligands that bear unwieldy C-13 substituents or nonsteroidal SARMs. A softened potential was applied by setting the van der Waals radii scaling to 0.7 for the receptor atoms with partial atomic charge $q \leq 0.25e$ and to 0.5 for ligand atoms with $q \leq 0.15e$.

Step (2) Prime Induced Fit. The top 20 poses generated by the softened-potential docking stage were selected according to their GlideScore and submitted to a full cycle of Prime protein refinement during the "Prime Induced Fit" step. During the refinement, OPLS parameters and a model of Generalized Born implicit solvent were used.[53,54] Residues temporarily mutated to alanine were returned to their original amino acid type. All residues within 5 Å of any ligand poses were chosen for further refinement steps consisting of side-chain conformational searches and minimizations. All complexes within a 30 kcal/mol window of the minimum energy structure were ranked by Prime energy (molecular mechanics plus solvation) before being submitted to the final step.

Step (3) Glide Redocking. The ligands that were minimized during the Initial Glide Docking stage were redocked against the receptor structures generated by the Prime Induced Fit step that were within 30.0 kcal/mol of the best structure and within the top 20 structures overall. The Glide Extra Precision (XP)[47] scoring function was used. At this stage, the receptor is treated rigidly (no softened potential applied) and van der Walls scaling factors were set to 1.0 and 0.8 for receptor and ligand atoms, respectively.

Step (4) Final Scoring. The IFD composite scoring function reported by Sherman[36] was used to rank the final AR/ligand complexes.

ASSOCIATED CONTENT

Supporting Information

Crystal structures of human Androgen Receptor Ligand Binding Domain (hARLBD) listed in alphabetic order along with relative PDB IDs, ligand identifiers, chemical structures, and ligand names. Primary citations for all structures are also included. This material is available free of charge via the Internet at http://pubs.acs.org.

AUTHOR INFORMATION

Corresponding Author

*Phone: (215) 596-8691. Fax: (215)596-8543. E-mail: r.zauhar@usciences.edu.

Author Contributions

The manuscript was written through contributions of all authors. All authors have given approval to the final version of the manuscript.

Notes

The authors declare no competing financial interest.

■ ACKNOWLEDGMENTS

The authors thank Dr. Vojislava Pophristic, Dr. Preston B. Moore, and Dr. Elia Eschenazi for their help in useful discussions. The West Center for Computational Chemistry and Drug Design is acknowledged for scientific support and the Schrödinger Staff for technical help and support.

■ ABBREVIATIONS

DHT, 5α-dihydrotestosterone; AR, Androgen Receptor; ARE, Androgen Response Elements; ARLBD, Androgen Receptor Ligand Binding Domain; CYP17, 17α-hydroxylase/17,20-lyase; CTD, C-terminal domain; DBD, DNA binding domain; hARLBD, human Androgen Receptor Ligand Binding Domain; HR, Hinge Region; IFD, Induced Fit Docking; LBD, ligand-binding domain; LBP, Ligand Binding Pocket; PCa, Prostate Cancer; R1881, Metribolone; NR, Nuclear Receptor; NSL, Non Steroidal Ligands; NTD, N-terminal domain; rmsd, Root Mean Square Deviation; SARM, Selective Androgen Receptor Modulator; SBDD, Structure-based Drug Design; SHRM, Selective Hormone Receptor Modulation; Testo, Testosterone

■ REFERENCES

(1) Heinlein, C. A.; Chang, C. Androgen Receptor in Prostate Cancer. *Endocr. Rev.* **2004**, *25*, 276−308.

(2) Roy, A. K.; Lavrovsky, Y.; Song, C. S.; Chen, S.; Jung, M. H.; Velu, N. K.; Bi, B. Y.; Chatterjee, B. Regulation of Androgen Action. *Vitam. Horm.* **1999**, *55*, 309−352.

(3) Mangelsdorf, D. J.; Thummel, C.; Beato, M.; Herrlich, P.; Schültz, G.; Umesono, K.; Blumberg, B.; Kastner, P.; Mark, M.; Chambon, P.; Evans, R. M. The Nuclear Receptor Superfamily: The Second Decade. *Cell* **1995**, *83*, 835−839.

(4) Claessens, F.; Denayer, S.; Van Tilborgh, N.; Kerkhofs, S.; Helsen, C.; Haelens, A. Diverse roles of androgen receptor (AR) domains in AR-mediated signaling. *Nucl. Recept. Signaling* **2008**, *6*, e008.

(5) Haelens, A.; Tanner, T.; Denayer, S.; Callewaert, L.; Claessens, F. The Hinge Region Regulates DNA Binding, Nuclear Translocation, and Transactivation of the Androgen Receptor. *Cancer Res.* **2007**, *67*, 4514−4523.

(6) Heinlein, C. A.; Chang, C. Androgen Receptor (AR) Coregulators: An Overview. *Endocr. Rev.* **2002**, *23*, 175−200.

(7) Margiotti, K.; Wafa, L. A.; Cheng, H.; Novelli, G.; Nelson, C. C.; Rennie, P. S. Androgen-Regulated Genes Differentially Modulated by the Androgen Receptor Coactivator L-Dopa Decarboxylase in Human Prostate Cancer Cells. *Mol. Cancer.* **2007**, *6*, 38.

(8) Smith, C. L.; O'Malley, B. W. Coregulator Function: A Key to Understanding Tissue Specificity of Selective Receptor Modulators. *Endocr. Rev.* **2004**, *25*, 45−71.

(9) Koochekpour, S. Androgen Receptor Signaling and Mutations in Prostate Cancer. *Asian J. Androl.* **2010**, *12*, 639−657.

(10) Berrevoets, C. A.; Umar, A.; Brinkmann, A. O. Antiandrogens: Selective Androgen Receptor Modulators. *Mol. Cell. Endocrinol.* **2002**, *198*, 97−103.

(11) Teodoro, M. L.; Kavraki, L. E. Conformational Flexibility Models for the Receptor in Structure Based Drug Design. *Curr. Pharm. Des.* **2003**, *9*, 1635−1648.

(12) Carlson, H. A. Protein Flexibility is an Important Component of Structure-Based Drug Discovery. *Curr. Pharm. Des.* **2002**, *8*, 1571−1578.

(13) Bisson, W. H.; Cheltsov, A. V.; Bruey-Sedano, N.; Lin, B.; Chen, J.; Goldberger, N.; May, L. T.; Christopoulos, A.; Dalton, J. T.; Sexton, P. M.; Zhang, X.-K.; Abagyan, R. Discovery of Antiandrogen Activity of Nonsteroidal Scaffolds of Marketed Drugs. *Proc. Natl. Acad. Sci. U. S. A.* **2007**, *104*, 11927−11932.

(14) Marhefka, C. A.; Moore, B. M., II; Bishop, T. C.; Kirkovsky, L.; Mukherjee, A.; Dalton, J. T.; Miller, D. D. Homology Modeling Using Multiple Molecular Dynamics Simulations and Docking Studies of the Human Androgen Receptor Ligand Binding Domain Bound to Testosterone and Nonsteroidal Ligands. *J. Med. Chem.* **2001**, *44*, 1729−1740.

(15) Njar, V. C. O.; Kato, K.; Nnane, I. P.; Grigoryev, D. N.; Long, B. J.; Brodie, A. M. H. Novel 17-Aazolyl Steroids, Potent Inhibitors of Human Cytochrome 17α-Hydroxylase/$C_{17,20}$-lyase (P45017α): Potential Agents for the Treatment of Prostate Cancer. *J. Med. Chem.* **1998**, *41*, 902−912.

(16) Grigoryev, D. N.; Long, B. J.; Nnane, I. P.; Njar, V. C. O.; Liu, Y.; Brodie, A. M. H. Effects of New 17α-Hydroxylase/$C_{17,20}$-Lyase Inhibitors of LNCaP Prostate Cancer Cell Growth *in Vitro* and *in Vivo*. *Br. J. Cancer* **1999**, *81*, 622−630.

(17) Long, B. J.; Grigoryev, D. N.; Nnane, I. P.; Liu, Y.; Ling, Y.-Z.; Brodie, A. M. H. Antiandrogenic Effects of Novel Androgen Synthesis Inhibitors on Hormone-dependent Prostate Cancer. *Cancer Res.* **2000**, *60*, 6630−6640.

(18) Njar, V. C. O.; Brodie, A. M. H. Inhibitors of 17alpha-Hydroxylase/17,20-Lyase (CYP17): Potential Agents for the Treatment of Prostate Cancer. *Curr. Pharm. Des.* **1999**, *5*, 163−180.

(19) Jarman, M.; Smith, H. J.; Nicholls, P. J.; Simons, C. Inhibitors of Enzymes of Androgen Biosynthesis: Cytochrome P450(17) alpha and 5 alpha-Steroid Reductase. *Nat. Prod. Rep.* **1998**, *15*, 495−512.

(20) O'Donnel, A.; Judson, I.; Dowsett, M.; Raynaud, F.; Dearnaley, D.; Mason, M; Harland, S.; Robbins, A.; Halbert, G.; Nutley, B.; Jarman, M. Hormonal Impact of the 17α-Hydroxylase/$C_{17,20}$-Lyase Inhibitor Abiraterone Acetate (CB7630) in Patients with Prostate Cancer. *Br. J. Cancer* **2004**, *90*, 2317−2325.

(21) Attard, G.; Reid, A. H. M.; Yap, T. A.; Raynaud, F.; Dowset, M.; Settatree, S.; Barret, M.; Parker, C.; Martins, V.; Folker, E.; Clark, J.; Cooper, C. S.; Kayne, S. B.; Dearnaley, D.; Lee, G.; De Bono, J. S. Phase I Clinical Trial of a Selective Inhibitor of CYP17, Abiraterone Acetate, Confirms That Castration-Resistant Prostate Cancer Commonly Remains Hormone Driven. *J. Clin. Oncol.* **2008**, *26*, 4563−4571.

(22) Handratta, V. D.; Vasaitis, T. S.; Njar, V. C. O.; Gediya, L. K.; Kataria, R.; Chopra, P.; Newman, D.; Farquhar, R.; Guo, Z.; Qiu, Y.; Brodie, A. M. H. Novel C-17-Heteroaryl Steroidal CYP17 Inhibitors/Antiandrogens: Synthesis, in Vitro Biological Activity, Pharmacokinetics, and Antitumor Activity in the LAPC4 Human Prostate Cancer Xenograft Model. *J. Med. Chem.* **2005**, *48*, 2972−2985.

(23) Schayowitz, A.; Sabnis, G.; Njar, V. C. O.; Brodie, A. M. H. Synergistic Effect of a Novel Antiandrogen, VN/124-1, and Signal Transduction Inhibitors in Prostate Cancer Progression to Hormone Independence *in Vitro*. *Mol. Cancer Ther.* **2008**, *7*, 121−132.

(24) Vasaitis, T.; Belosay, A.; Schayowitz, A.; Khandelwal, A.; Chopra, P.; Gediya, L. K.; Guo, Z.; Fang, H.-B.; Njar, V. C. O.; Brodie, A. M. H. Androgen Receptor Inactivation Contributes to Antitumor Efficacy of CYP17 Inhibitor VN/124-1 in Prostate Cancer. *Mol. Cancer Ther.* **2008**, *7*, 2348−2357.

(25) Montgomery, R. B.; Taplin, M. E. ARMOR1: Study of TOK-001 to Treat Castration Resistant Prostate Cancer, 2009. ClinicalTrials.gov Web Site. http://clinicaltrials.gov/ct2/show/study/NCT00959959 (accessed 08/09/2011).

(26) TOKAI PHARMACEUTICALS, Cambridge, MA 02142. http://www.tokaipharma.com/ (accessed May 1, 2011).

(27) DeVore, N. M.; Scott, E. E. Structures of cytochrome P450 17A1 with prostate cancer drugs abiraterone and TOK-001. *Nature* **2012**, *482*, 116−119.

(28) RCSB Protein Data Bank. http://www.rcsb.org/pdb (accessed May 1, 2011).

(29) Estebanez-Perpina, E.; Arnold, L. A.; Nguyen, P.; Rodrigues, E. D.; Mar, E.; Bateman, R.; Pallai, P.; Shokat, K. M.; Baxter, J. D.; Guy, R. K.; Webb, P.; Fletterick, R. J. A Surface on the Androgen Receptor That Allosterically Regulates Coactivator Binding. *Proc. Natl. Acad. Sci. U. S. A.* **2007**, *104*, 16074−16079.
(30) Pereira de Jésus-Tran, K.; Côté, P. L.; Cantin, L.; Blanchet, J.; Labrie, F.; Breton, R. Comparison of Crystal Structures of Human Androgen Receptor Ligand-Binding Domain Complexed with Various Agonists Reveals Molecular Determinants Responsible for Binding Affinity. *Protein Sci.* **2006**, *15*, 987−999.
(31) He, B.; Gampe, R. T., Jr.; Kole, A. J.; Hnat, A. T.; Stanley, T. B.; An, G.; Stewart, E. L.; Kalman, R. I.; Minges, J. T.; Wilson, E. M. Structural Basis for Androgen Receptor Interdomain and Coactivator Interactions Suggests a Transition in Nuclear Receptor Activation Function Dominance. *Mol. Cell* **2004**, *16*, 425−438.
(32) Matias, P. M.; Carrondo, M. A.; Coelho, R.; Thomaz, M.; Zhao, X. Y.; Wegg, A.; Crusius, K.; Egner, U.; Donner, P. Structural Basis for the Glucocorticoid Response in a Mutant Human Androgen Receptor (AR^{ccr}) Derived from an Androgen-Independent Prostate Cancer. *J. Med. Chem.* **2002**, *45*, 1439−1446.
(33) Bohl, C. E.; Miller, D. D.; Chen, J.; Bell, C. E.; Dalton, J. T. Structural Basis for Accommodation of Nonsteroidal Ligands in the Androgen Receptor. *J. Biol. Chem.* **2005**, *280*, 37747−37754.
(34) Bohl, C. E.; Wu, Z.; Chen, J.; Mohler, M. L.; Yang, J.; Hwang, D. J.; Mustafa, S.; Miller, D. D.; Bell, C. E.; Dalton, J. Effect of B-Ring Substitution Pattern on Binding Mode of Propionamide Selective Androgen Receptor Modulators. *Bioorg. Med. Chem. Lett.* **2008**, *18*, 5567−5570.
(35) Schrödinger Suite 2010 Induced Fit Docking protocol; Glide version 5.6, Schrödinger, LLC, New York, NY, 2010; Prime version 2.2, Schrödinger, LLC, New York, NY, 2010.
(36) Sherman, W.; Day, T.; Jacobson, M. P.; Friesner, R. A.; Farid, R. Novel Procedure for Modeling Ligand/Receptor Induced Fit Effects. *J. Med. Chem.* **2006**, *49*, 534−553.
(37) Sherman, W.; Beard, H. S.; Farid, R. Use of an Induced Fit Receptor Structure in Virtual Screening. *Chem. Biol. Drug Des.* **2006**, *67*, 83−84.
(38) Farid, R.; Day, T.; Friesner, R. A.; Pearlstein, R. A. New Insights about HERG Blockade Obtained from Protein Modeling, Potential Energy Mapping, and Docking Studies. *Bioorg. Med. Chem.* **2006**, *14*, 3160−3173.
(39) Gao, W.; Bohl, C. E.; Dalton, J. T. Chemistry and Structural Biology of Androgen Receptor. *Chem. Rev.* **2005**, *105*, 3352−3370.
(40) Cantin, L.; Faucher, F.; Couture, J. F.; De Jesus-Tran, K. P.; Legrand, P.; Ciobanu, L. C.; Frechette, Y.; Labrecque, R.; Singh, S. M.; Labrie, F.; Breton, R. Structural Characterization of the Human Androgen Receptor Ligand-binding Domain Complexed with EM5744, a Rationally Designed Steroidal Ligand Bearing a Bulky Chain Directed towards Helix 12. *J. Biol. Chem.* **2007**, *282*, 30910−30919.
(41) Bohl, C. E.; Wu, Z.; Miller, D. D.; Bell, C. E.; Dalton, J. T. Crystal Structure of the T877A Human Androgen Receptor Ligand-Binding Domain Complexed to Cyproterone Acetate Provides Insights for Ligand-Induced Conformational Changes and Structure-Based Drug-Design. *J. Biol. Chem.* **2007**, *282*, 13648−13655.
(42) Van de Wijngaart, D. J.; Molier, M.; Lusher, S. J.; Hersmus, R.; Jenster, G.; Trapman, J.; Dubbink, H. J. Sytematic Structure-Function Analysis of Androgen Receptor Leu^{701} Mutants Explains the Properties of the Prostate Cancer Mutant L701H. *J. Biol. Chem.* **2010**, *285*, 5097−5105.
(43) Bohl, C. E.; Gao, W.; Miller, D. D.; Bell, C. E.; Dalton, J. T. Structural Basis for Antagonism and Resistance of Bicalutamide in Prostate Cancer. *Proc. Natl. Acad. Sci. U. S. A.* **2005**, *102*, 6201−6206.
(44) Glide, version 5.6, Schrödinger, LLC, New York, NY, 2010.
(45) Friesner, R. A.; Banks, J. L.; Murphy, R. B.; Halgren, T. A.; Klicic, J. J.; Mainz, D. T.; Repasky, M. P.; Knoll, E. H.; Shelly, M.; Perry, J. K.; Shaw, D. E.; Francis, P.; Shenkin, P. S. Glide: A New Approach for Rapid, Accurate Docking and Scoring. 1. Method and Assessment of Docking Accuracy. *J. Med. Chem.* **2004**, *47*, 1739−49.
(46) Halgren, T. A.; Murphy, R. B.; Friesner, R. A.; Behard, H. S.; Frye, L. L.; Pollard, W. T.; Banks, J. L. Glide: A New Approach for Rapid, Accurate Docking and Scoring. 2. Enrichment Factors in Database Screening. *J. Med. Chem.* **2004**, *47*, 1750−1759.
(47) Friesner, R. A.; Murphy, R. B.; Repasky, M. P.; Frye, L. L.; Greenwood, J. R.; Halgren, T. A.; Sanschagrin, P. C.; Mainz, D. T. Extra Precision Glide: Docking and Scoring Incorporating a Model of Hydrophobic Enclosure for Protein-Ligand Complexes. *J. Med. Chem.* **2006**, *49*, 6177−6196.
(48) Prime, version 2.2, Schrödinger, LLC, New York, NY, 2010.
(49) Jacobson, M. P.; Pincus, D. L.; Rapp, C. S.; Day, T. J. F.; Honig, B.; Shaw, D. E.; Friesner, R. A. A Hierarchical Approach to All-Atom Protein Loop Prediction. *Proteins* **2004**, *55*, 351−367.
(50) Jacobson, M. P.; Friesner, R. A.; Xiang, Z.; Honig, B. On the Role of the Crystal Environment in Determining Protein Side-chain Conformations. *J. Mol. Biol.* **2002**, *320*, 597−608.
(51) Jorgensen, W. L.; Maxwell, D. S.; Tirado-Rives, J. Development and Testing of the OPLS All-Atom Force Field on Conformational Energetics and Properties of Organic Liquids. *J. Am. Chem. Soc.* **1996**, *118*, 11225−11236.
(52) Kaminski, G. A.; Friesner, R. A.; Tirado-Rives, J.; Jorgensen, W. L. Evaluation and Reparametrization of the OPLS-AA Force Field for Proteins via Comparison with Accurate Quantum Chemical Calculations on Peptides. *J. Phys. Chem. B* **2001**, *105*, 6474−6487.
(53) Ghosh, A.; Rapp, C. S.; Friesner, R. A. Generalized Born Model Based on a Surface Integral Formulation. *J. Phys. Chem. B* **1998**, *102*, 10983−10990.
(54) Gallicchio, E.; Zhang, L. Y.; Levy, R. M. The SGB/NP Hydration Free Energy Model Based on the Surface Generalized Born Solvent Reaction Field and Novel Non-Polar Hydration Free Energy Estimators. *J. Comput. Chem.* **2002**, *23*, 517−529.
(55) Brzozowski, A. M.; Pike, A. C.; Dauter, Z.; Hubbard, R. E.; Bonn, T.; Engstrom, O.; Öhman, L.; Greene, G. L.; Gustafsson, J. A.; Carlquist, M. Molecular Basis for Agonism and Antagonism in the Oestrogen Receptor. *Nature* **1997**, *389*, 753−758.
(56) Gao, W. Peptide Antagonists of the Androgen Receptor. *Curr. Pharm. Des.* **2010**, *16*, 1106−1113.
(57) Maestro, version 9.1, Schrödinger, LLC, New York, NY, 2010.
(58) Impact, version 5.6, Schrödinger, LLC, New York, NY, 2005.
(59) LigPrep, version 2.4, Schrödinger, LLC, New York, NY, 2010.
(60) Epik, version 2.1, Schrödinger, LLC, New York, NY, 2010.
(61) Shelley, J. C.; Cholleti, A.; Frye, L. L.; Greenwood, J. R.; Timlin, M. R.; Uchiyama, M. Epik: a Software Program for pK(a) Prediction and Protonation State Generation for Drug-Like Molecules. *J. Comput.-Aided Mol. Des.* **2007**, *21*, 681−691.
(62) Greenwood, J. R.; Calkins, D.; Sullivan, A. P.; Shelley, J. C. Towards the Comprehensive, Rapid, and Accurate Prediction of the Favorable Tautomeric States of Drug-Like Molecules in Aqueous Solution. *J. Comput.-Aided Mol. Des.* **2010**, *24*, 591−604.
(63) Estebanez-Perpina, E.; Moore, J. M. R.; Mar, E.; Delgado-Rodrigues, E.; Nguyen, P.; Baxter, J. D.; Buehrer, B. M.; Webb, P.; Fletterick, R. J.; Guy, R. K. The Molecular Mechanisms of Coactivator Utilization in Ligand-dependent Transactivation by the Androgen Receptor. *J. Biol. Chem.* **2005**, *280*, 8060−8068.
(64) Askew, E. B.; Gampe, R. T.; Stanley, T. B.; Faggart, J. L.; Wilson, E. M. Modulation of Androgen Receptor Activation Function 2 by Testosterone and Dihydrotestosterone. *J. Biol. Chem.* **2007**, *282*, 25801−25816.
(65) Zhou, X. E.; Suino-Powell, K. M.; Li, J.; He, Y.; Mackeigan, J. P.; Melcher, K.; Yong, E. L.; Xu, H. E. Identification of SRC3/AIB1 as a Preferred Coactivator for Hormone-activated Androgen Receptor. *J. Biol. Chem.* **2010**, *285*, 9161−9171.